Kyba, C., Küster, T., Sánchez de Miguel, A., Baugh, K., Jechow, A., Hölker, F., Bennie, J., Elvidge, C. D., Gaston, K. J., Guanter, L. (2017): Artificially lit surface of Earth at night increasing in radiance and extent. - *Science Advances*, *3*, 11.

DOI: http://doi.org/10.1126/sciadv.1701528

ENVIRONMENTAL SCIENCES

Artificially lit surface of Earth at night increasing in radiance and extent

Christopher C. M. Kyba,[1,2]* Theres Kuester,[1] Alejandro Sánchez de Miguel,[3,4†] Kimberly Baugh,[5] Andreas Jechow,[1,2] Franz Hölker,[2] Jonathan Bennie,[6] Christopher D. Elvidge,[7] Kevin J. Gaston,[8] Luis Guanter[1]

A central aim of the "lighting revolution" (the transition to solid-state lighting technology) is decreased energy consumption. This could be undermined by a rebound effect of increased use in response to lowered cost of light. We use the first-ever calibrated satellite radiometer designed for night lights to show that from 2012 to 2016, Earth's artificially lit outdoor area grew by 2.2% per year, with a total radiance growth of 1.8% per year. Continuously lit areas brightened at a rate of 2.2% per year. Large differences in national growth rates were observed, with lighting remaining stable or decreasing in only a few countries. These data are not consistent with global scale energy reductions but rather indicate increased light pollution, with corresponding negative consequences for flora, fauna, and human well-being.

INTRODUCTION

Continued improvement in the luminous efficacy of light sources and increases in gross domestic product (GDP) have resulted in tremendous growth in artificial light use over several centuries (*1*). Historically, lighting has been subject to a strong rebound effect, in which increases in luminous efficacy result in correspondingly greater light use rather than energy savings (*2*). Regardless of historical or geographical context, humans tend to use as much artificial light as they can buy for ~0.7% of GDP (*3*). Outdoor lighting became commonplace with the introduction of electric light and grew at an estimated rate of 3 to 6% per year during the second half of the 20th century (*4*). As a result, the world has experienced widespread "loss of the night," with half of Europe and a quarter of North America experiencing substantially modified light-dark cycles (*5*).

A critical question for sustainable development is whether the use of outdoor light will continue to grow exponentially or whether developed countries are nearing saturation in demand (*3*). In addition to the possibility that the existing light levels are already sufficient for any desired visual task, factors that reduce demand include greater public recognition of the unintended ecological (*6*) and astronomical (*5*, *7*) impacts of outdoor light pollution, official warnings that overexposure to artificial light may be affecting human sleep and health (*8*), efforts to transition to a sustainable society with decreased electricity demand (*9*), the desire of local governments to reduce the costs of lighting (*10*), and the establishment of protected "dark sky" areas (*11*). If demand saturation has not been reached, then the increasing luminous efficacy made possible by the solid-state lighting revolution (*12*) will increase light emissions instead of saving energy.

Changes in outdoor lighting can be measured on the global scale only via Earth-observing satellites, but no calibrated satellite sensor has made global observations of night lights until recently. The well-known older images of Earth at night (*13*) were based on an uncalibrated sensor from a defense satellite [Defense Meteorological Satellite Program (DMSP)], which had frequent and unrecorded changes in sensor gain. Despite this drawback, there have been attempts to use statistical methods to try to intercalibrate the time series. These methods sometimes rely on questionable assumptions, such as the assumption that Sicily experienced no changes in lighting over a 15-year period (*14*). In addition to the lack of an on-board radiance calibration, DMSP experienced saturation in cities and had low (8 bit) radiometric resolution and an intrinsic spatial resolution of 5 km (*15*). Nevertheless, the inherent connection between artificial light and human activity means that DMSP data display strong correlations with many socioeconomic factors (*16*).

Although considerable research has been done using DMSP time series, most analyses have been focused on other remotely sensed factors [for example, human settlement, socioeconomic activity, and detection of fishing vessels (*17*)] and have not reported on trends in lighting itself. The few lighting studies that have done so were on the national [for example, 4% annual increase in Spain (*18*)] or continental scale [for example, (*19*)] or else examined only a specific class of lighting [for example, (*14*)]. The official radiance-calibrated DMSP time series of the National Oceanic and Atmospheric Administration (NOAA) showed little change in the sum of lights of several large cities, but the intercalibration was based on the assumption that the lights of Los Angeles did not change over the period of 1996–2010 (*20*). In contrast, a recent analysis using a different methodology found an increase in global lights of a factor of 2 from 1992 to 2013 (~ 3.5% per year) (*21*). However, because of the limitations of the DMSP, and particularly the saturation in city centers, many analyses have been limited to change in lit area rather than change in radiance.

The Visible Infrared Imaging Radiometer Suite Day-Night Band (VIIRS DNB) came online just as outdoor use of light-emitting diode (LED) lighting began in earnest (*22*). This sensor provides the first-ever global calibrated nighttime radiance measurements in a spectral band of 500 to 900 nm, which is close to the visible band, with a much higher radiometric sensitivity than the DMSP, and at a spatial resolution of near 750 m (*15*). This improved spatial resolution allows neighborhood (rather than city or national) scale changes in lighting to be investigated for the first time (*23*).

[1]GFZ German Research Centre for Geosciences, Potsdam 14473, Germany. [2]Leibniz Institute of Freshwater Ecology and Inland Fisheries (IGB), Berlin 12587, Germany. [3]Instituto de Astrofísica de Andalucía, Glorieta de la Astronomía s/n, Granada C.P. 18008, Spain. [4]Dept. Astrofísica y CC. de la Atmósfera, Universidad Complutense de Madrid, Madrid 28040, Spain. [5]Cooperative Institute for Research in the Environmental Sciences, University of Colorado, Boulder, CO 80309, USA. [6]Centre for Geography, Environment and Society, University of Exeter, Penryn TR10, UK. [7]National Oceanic and Atmospheric Administration, Boulder, CO 80305, USA. [8]Environment and Sustainability Institute, University of Exeter, Penryn, Cornwall TR10 9FE, UK.
*Corresponding author. Email: kyba@gfz-potsdam.de
†Present address: Environment and Sustainability Institute, University of Exeter, Penryn, Cornwall TR10 9FE, UK.

RESULTS

The cloud-free DNB data show that over the period of 2012–2016, both lit area and the radiance of previously lit areas increased in most countries (Fig. 1) in the 500–900-nm range, with global increases of 2.2% per year for lit area and 2.2% per year for the brightness of continuously lit areas (see Materials and Methods). Overall, the radiance of areas lit above 5 nWcm^{-2} sr^{-1} increased by 1.8% per year. These factors decreased in very few countries, including several experiencing warfare [for example, Yemen (*24*) and Syria]. They were also stable in only a few countries, interestingly including some of the world's brightest (for example, Italy, Netherlands, Spain, and the United States). With few exceptions, growth in lighting occurred throughout South America, Africa, and Asia. Because the analysis of lit area and total radiance is not subject to a stability criterion, transient lights such as wildfires can cause large fluctuations. Australia experienced a major decrease in lit area from 2012 to 2016 for this reason (Figs. 1A and 2). However, fire-lit areas failed the stability test and were therefore not included in the radiance change analysis (Fig. 1B). A small number of countries have "no data" because of either their extreme latitude (Iceland) or the lack of observed stable lights above 5 nWcm^{-2} sr^{-1} in the cloud-free composite (for example, Central African Republic).

Brightly lit areas are uncommon: For most countries, over half of the national light emission above the analysis threshold came from areas lit below 20 nWcm^{-2} sr^{-1} (Fig. 3, A and B, and figs. S1 to S3). For context, small towns in the American West with populations of several hundreds are typically slightly above the 5 nWcm^{-2} sr^{-1} threshold, whereas the radiance observed at international airports is typically ~150 nWcm^{-2} sr^{-1} (*23*). The area-radiance curve is often approximately power-law, but the shape and the slope are not consistent across countries (figs. S4 to S27; see the study of Small *et al.* (*25*) for a discussion

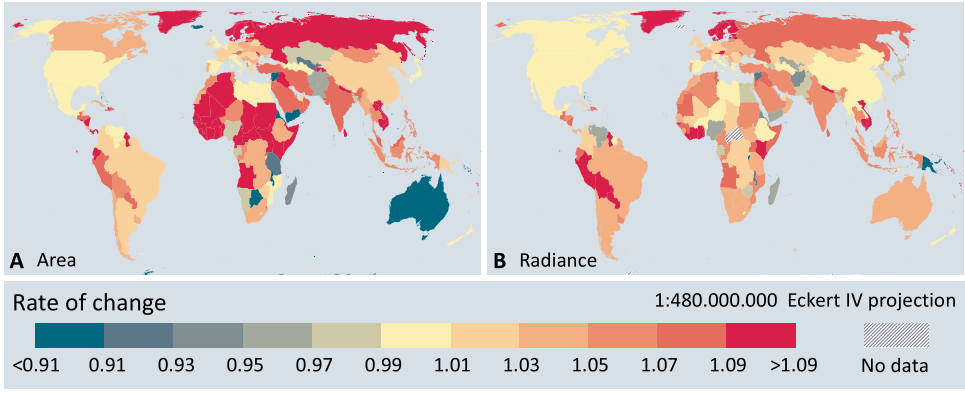

Fig. 1. Geographic patterns in changes in artificial lighting. Changes are shown as an annual rate for both lit area (**A**) and radiance of stably lit areas (**B**). Annual rates are calculated based on changes over the four year period, that is, $\sqrt[4]{A_{2016}/A_{2012}}$, where A_{2016} is the lit area observed in 2016. See fig. S28 for total radiance change instead of stable light radiance change.

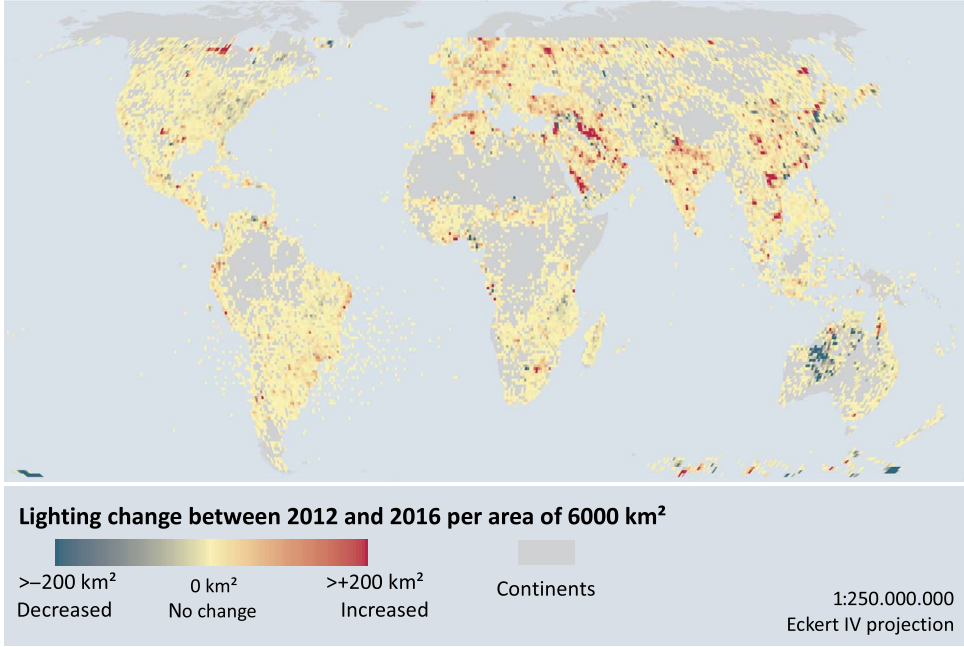

Fig. 2. Absolute change in lit area from 2012 to 2016. Pixels increasing in area are shown as red, pixels decreasing in area are shown as blue, and pixels with no change in area are shown as yellow. Each pixel has a near-equal area of 6000 ± 35 km^2. To ease interpretation, the color scale cuts off at 200 km^2, but some pixels had changes of up to ±2000 km^2.

of how these relationships may emerge naturally, and compare the studies of Small and Elvidge (*26*) for DMSP and Kuechly *et al.* (*27*) for higher-resolution aerial photos). For example, compared to China, the United States has twice as much area illuminated with radiances in the range of 5 to 6.1 nWcm^{-2} sr^{-1} but nearly 20 times as much area illuminated in the range of 132 to 162 nWcm^{-2} sr^{-1}. The shape difference is even more striking for Bolivia and Pakistan. In many countries, there is little or no area lit above 100 nWcm^{-2} sr^{-1}.

The global 9.1% increase in stable light radiance from 2012 to 2016 (2.2% per year) applies nearly independently of radiance in 2014 (Fig. 3C). However, in some individual countries, radiance change was not uniform across the 2014 radiance classes. In the UK, for example, the rate of lighting change was positively correlated with 2014 radiance (fig. S26). Nevertheless, even large increases in bright areas have relatively little effect on the country-level radiance change, because these areas typically account for a small fraction of the national light emission (Fig. 3B and figs. S1 to S27).

Summed national per capita and total light emissions above the 5 nWcm^{-2} sr^{-1} threshold are correlated with per capita and national GDP (Spearman rank-order correlation coefficient of 0.76 and 0.85, respectively, $P \ll 0.001$; Fig. 4, A and B). This confirms the results of earlier studies using DMSP data [for example, the studies of Doll *et al.* (*28*) and Nordhaus and Chen (*29*)]. Nevertheless, there are large (up to order of magnitude) differences between countries with similar wealth, and the relationship between per capita light and GDP appears to be nonlinear (Fig. 4A). Note that for a small number of northern countries (for example, Finland), the national sum of lights does not include lights located above 60° North. The size of changes in lights and changes in GDP was larger in poorer countries and smaller in wealthier countries. For the median country, the sum of total radiance grew by 15% from 2012 to 2016, which is quite close to the median country's GDP increase (13%) over the same time frame. However, the Spearman rank-order correlation between GDP and light change (Fig. 4D) was only 0.17 ($P = 0.05$). The Spearman rank-order correlation between GDP and lit area change (Fig. 4C) was slightly larger, at 0.24 ($P = 0.006$).

Many large cities had decreases in DNB radiance in the city center but increases in outlying areas. These decreases can often be directly attributed to replacement of older lamps with LEDs. This is vividly demonstrated by photographs of Milan, Italy, taken by astronauts on the International Space Station in 2012 and 2015 (Fig. 5, A and B). The

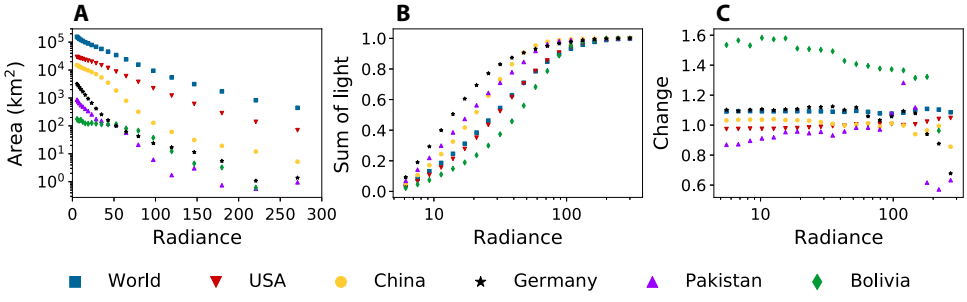

Fig. 3. Patterns in lit area, radiance, and lighting change for the world and five selected countries. (**A**) The 2014 lit area (in km^2) for each (logarithmically spaced) bin of radiance in nWcm^{-2} sr^{-1}. (**B**) Normalized cumulative distribution of light in 2016 (that is, what fraction of the total light is emitted below the given radiance). (**C**) Mean change in radiance from 2012 to 2016 for each bin.

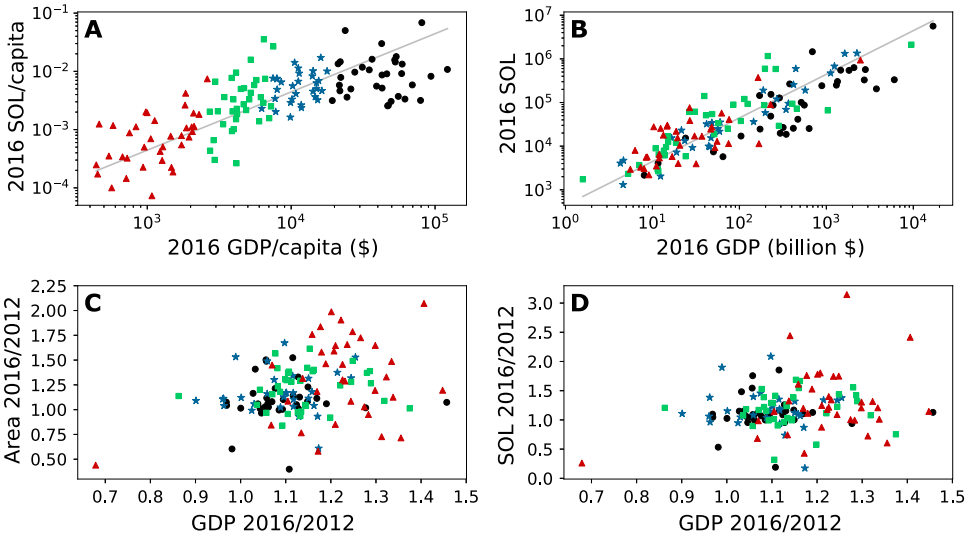

Fig. 4. Relationships between light and economic parameters. (**A**) National sum of lights (SOL) per capita compared to per capita GDP, (**B**) sum of lights versus national GDP, (**C**) change in lit area from 2012 to 2016 versus change in GDP (one outlier not shown), and (**D**) change in sum of lights from 2012 to 2016 versus change in GDP. Colors and symbols indicate per capita GDP in 2016: <$2000 (red triangles), $2000 to $6000 (green squares), $6000 to $17,000 (blue stars), and >$17,000 (black circles). Solid lines show an extrapolation based on the value of the median country.

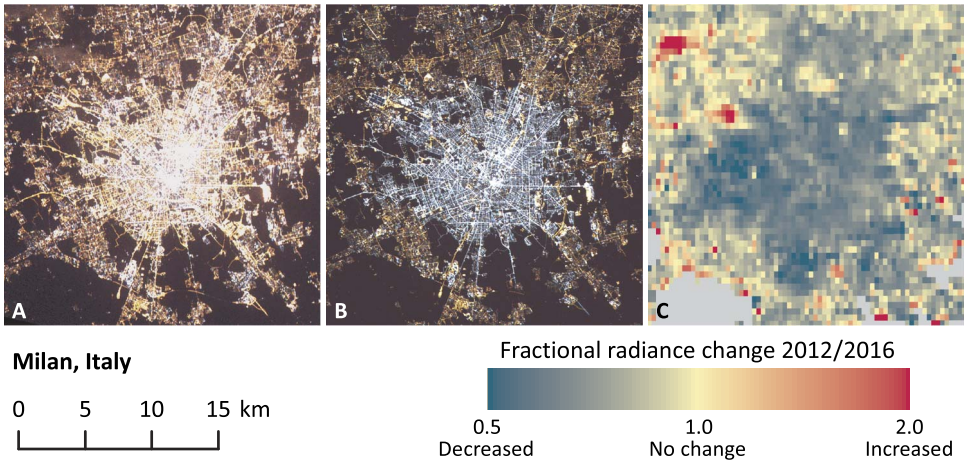

Fig. 5. Change in lighting technology in Milan, Italy, observed from space. Color astronaut photographs from 2012 (**A**) and 2015 (**B**) courtesy of the Earth Science and Remote Sensing Unit, NASA Johnson Space Center, with identification and georeferencing by the European Space Agency, the International Astronomical Union, and Cities at Night (*48*). (**C**) Change from 2012 to 2016 in the DNB radiance band.

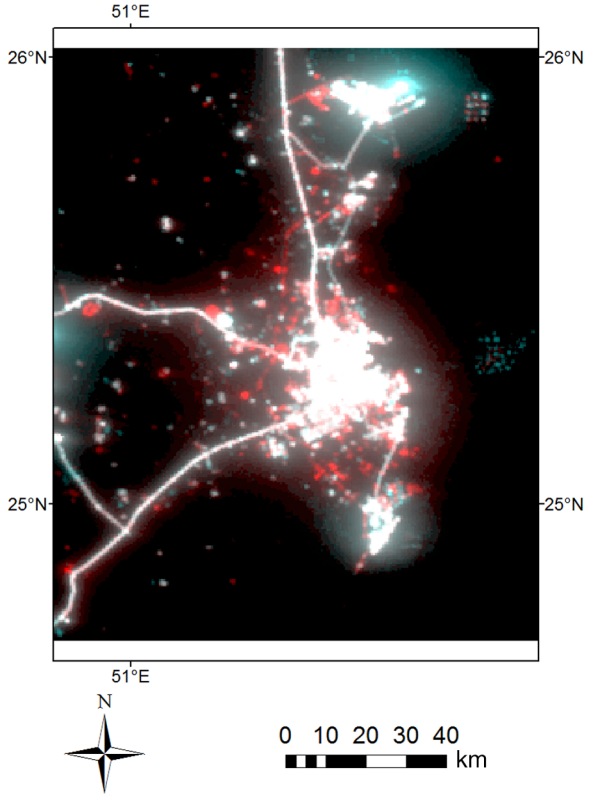

Fig. 6. Expansion of DNB lighting from September 2012 (cyan) to September 2016 (red) in Doha, Qatar. Newly lit areas are expressed as bright red, as they were not lit (black) in 2012.

street lights in the city changed from yellow/orange (sodium vapor) to white (LED), whereas the surrounding areas remained yellow/orange. As a result, the radiance observed by the DNB decreased (Fig. 5C) because of the sensor's lack of sensitivity to light in the range of 400 to 500 nm (*23*). Similar transitions can be seen (and verified with newspaper accounts) in many cities worldwide.

Increases in radiance in areas around cities may result from several processes. In many cases, cities expand into new areas, causing their edges (which were previously only partly urbanized) to become brighter. In other cases, radiance increase may be due to expansion of electrification or to increasing wealth in adjacent areas. Finally, some of the light observed by the satellite is not direct but rather scattered by the atmosphere. For very bright cities, this causes a glow over adjacent areas that have little or no lighting. Transitions to LED lighting greatly increase this "skyglow," because the clear sky predominantly scatters short-wavelength light (*30*). This effect would be considerably more noticeable if the DNB was sensitive to light below 500 nm. Similarly, whereas decreases in city center radiance in the DNB band likely indicate absolute energy reductions (see Materials and Methods), white LED transitions will often increase the skyglow experienced on the ground (*30*–*32*).

DISCUSSION

Major arguments for transition to LEDs for outdoor lighting are cost savings and reductions in energy consumption (*9*). These goals have been realized in many cities that have switched to LED street lights, and therefore, decreases in observed DNB radiance likely indicate local energy savings. However, on the global (and often national) scale, these local decreases are outweighed by increases in radiance in other areas, most likely because of additional lighting being installed. This should not be surprising, because decreases in cost allow increased use of light in areas that were previously unlit, moderately lit, or lit only during the early evening hours. The "energy saving" effects of outdoor LED lighting for country-level energy budgets are therefore smaller than might be expected from the increase in luminous efficacy compared to older lamps (*33*).

The large differences in per capita light use compared to per capita GDP (Fig. 4A) suggest that in brightly lit countries, major decreases in energy consumption for outdoor lighting could potentially be achieved through reduced light use. The extremely large differences in per capita light use in Germany and the United States reported in the study of Kyba *et al.* (*23*) and observed again here (Fig. 3, A and B) demonstrate that prosperity, safety, and security can be achieved with conservative light use. This has also been shown on local scales: Demonstration

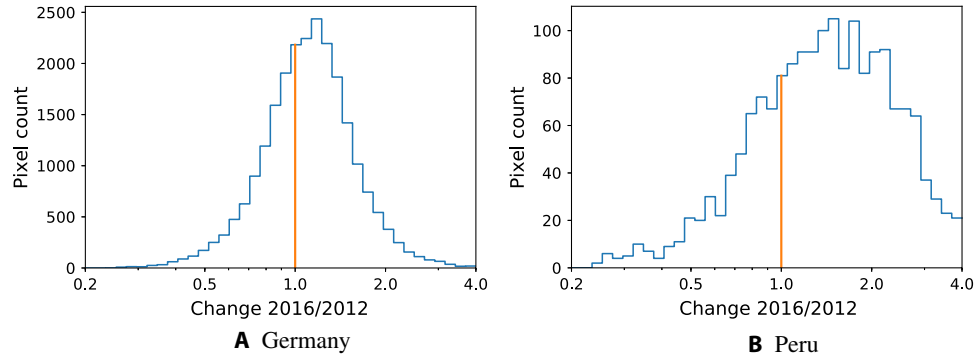

Fig. 7. Comparison of radiance changes from 2012–2016 in dimly lit areas of Germany and Peru. Histograms of radiance changes of pixels in the 5 to 6.1 nWcm^{-2} sr^{-1}bin for Germany (**A**) and rapidly brightening Peru (**B**). Pixels were assigned to this bin on the basis of their radiance in 2014. The vertical line shows the value of 1 (no change from 2012 to 2016).

projects have shown that LEDs can allow approximately order-of-magnitude reductions in illuminance compared to current practice without compromising user acceptance (*34*). In addition, lighting can be reduced or turned off late at night without compromising safety in the moderately lit places responsible for most of the artificial light emissions (*10*).

Major (factor of 2 or more) reductions in the energy cost and environmental impact of lighting should be accompanied by large absolute decreases in light emissions observable from space. The fact that the median country's 15% increase in lighting from 2012 to 2016 nearly matched the median 13% increase in GDP suggests that outdoor light use remains subject to a large rebound effect on the global scale. Therefore, the results presented here are inconsistent with the hypothesis of large reductions in global energy consumption for outdoor lighting because of the introduction of solid-state lighting. The correlation between GDP and light increase at the national scale is likely modest because of the relatively short-term nature of the data set, compared to the ~20-year time window for replacement of city street lights. The size of the outdoor lighting rebound effect should therefore be re-examined when a longer time series of lights and GDP becomes available. Restricting the analysis to stable electric lighting, and lowering the analysis threshold from 5 nWcm^{-2} sr^{-1} to the smallest practical value, would also likely improve these correlations.

In the near term, it appears that artificial light emission into the environment will continue to increase, further eroding Earth's remaining land area that experiences natural day-night light cycles. This is concerning, because artificial light is an environmental pollutant. In addition to threatening the 30% of vertebrates and more than 60% of invertebrates that are nocturnal (*35*), outdoor artificial light also affects plants and microorganisms (*36*, *37*) and is increasingly suspected of affecting human health (*8*, *38*). In the longer term, perhaps the demand for dark skies and unlit bedrooms will begin to outweigh the demand for light in wealthy countries, leading to an "environmental Kuznets curve" for outdoor light. The nonlinearity between per capita light emission and GDP is reminiscent of such a relationship (Fig. 4A). If this is the case, then it will be readily apparent in the continued time series of satellites observing artificial light at night.

MATERIALS AND METHODS

Three analyses were conducted: an "area change" analysis, a "total radiance change" analyses, and a "stable light radiance change" analysis. All three analyses compare relative rather than absolute changes to facilitate comparisons.

The area change analysis measured the total area that was lit above a certain radiance threshold in 2012 and 2016. In this analysis, the radiance of individual pixels was reduced to a single bit (lit or unlit, based on a cut of 5 nWcm^{-2} sr^{-1}). Areas that increased in radiance to cross the threshold in 2016 therefore increased the lit area compared to 2012, whereas increases in radiance in city centers that were already lit in 2012 had no impact on the lit area. Transient and natural light sources such as wildfires necessarily affected the area change analysis. This is because if a light is only present in the 2012 or 2016 data set, then there is no way to know whether it was a formerly permanent light that turned off after 2012, a new permanent light that turned on in 2016, or a transient light in one of the two years. [NOAA is working on annual "stable lights" composites that remove firelight on the basis of infrared observations (*39*), but these are not yet published for all years, and the outlier removal method it is based on cannot be applied to monthly data.] A selection of maps showing area changes at high resolutions using the same data but a different analysis were recently published by Nelson (*40*).

The total radiance change analysis measured the national sum of the radiance of all pixels that were above 5 nWcm^{-2} sr^{-1} in 2012, 2016, or both 2012 and 2016 (SOL in Fig. 4). This means that the area under consideration is the same as in the area change analysis, and an identical area is considered in the two years. As in the area change analysis, transient light sources such as fire were included in the total.

The stable light radiance change analysis measured how radiance changed in areas continuously lit with relatively stable lights from 2012 to 2016. Transient and wildfire lights were removed by checking that the area was lit above a 5 nWcm^{-2} sr^{-1} threshold in the entire period of 2012–2016 and that the change in radiance from 2012 to 2016 did not exceed a set value (details below). Areas were binned according to their radiance in 2014 in order to test whether, for example, city centers have different trends compared to more modestly lit areas. Because transient and natural light sources were removed, the study area used in the radiance change analysis was smaller than the area observed in the other two analyses. Wildfires outside artificially illuminated areas in a single year should therefore have no effect on the stable light radiance change analysis.

The DNB cloud-free monthly composites for the month of October in 2012–2016 were downloaded from NOAA (*41*). These data include only overpasses for which clouds were not present (based on observations by infrared channels on the same instrument), and the total number of overpasses therefore differs between pixels. In a few areas, some pixels are so persistently covered by clouds that no cloud-free observations are available in a given month. In this case, the area was

removed from all the analyses presented here. October is a particularly good month for comparisons of nighttime lights data for several reasons. Stray light does not affect the observation at high latitudes in Europe, and these areas are less likely to experience snow than later in the year (however, note that Austria was particularly affected by snow in October 2016). Seasonal changes in DNB observations were recently discussed by Levin and Zhang (*42*). In addition to the effect of snow, they found a negative relationship between the number of cloud-free observations and the radiance of cities. This should be further investigated, but we note that it could potentially be due to a complete lack of cloud-free observations in some of their study areas, or perhaps more likely, an interaction in their model between location, cloud cover, and season. Long-term changes in the radiometric calibration of the DNB itself are well understood and corrected (*43*).

The DNB monthly composites report the surface radiance in equal-angle pixels of 15 arc sec in latitude and longitude. Rather than reprojecting these data onto an equal-area map, we assigned a weight to each pixel on the basis of its surface area (assuming a spherical Earth). To reject auroral light, we cropped images to cover only the region of 60°S to 60°N (from the original 65°S to 75°N). Some auroral light remained over the ocean in the Southern Hemisphere (Fig. 2), so the area below 48° was removed from the analyses with the exception of 50°W to 80°W. An array containing the surface area dA of the 15″ pixels was generated in Python according to

$$dA = R_{\text{Earth}}^2 \cos\theta \, d\theta d\phi \tag{1}$$

$$A = R_{\text{Earth}}^2 \int_{\theta_1}^{\theta_2} \cos\theta \, d\theta \int_{\phi_1}^{\phi_2} d\phi \tag{2}$$

$$A = R_{\text{Earth}}^2 \left[\sin\theta \right]_{\theta_1}^{\theta_2} \left[\phi \right]_{\phi_1}^{\phi_2} \tag{3}$$

where θ is the latitude in radians (that is, θ = 0 at the equator) and ϕ is the longitude.

The stable light radiance change analysis examines how radiance changed from 2012 to 2016 in dimly, moderately, and brightly lit areas. To do this, and to allow the generation of histograms, we used the pixel radiance (R) in the 2014 composite to assign each pixel a radiance class (bin), with logarithmically growing width. The low edges of these bins were assigned as

$$R_{\text{left}} = \log_{10}(R_{\text{hi}}) - \log_{10}(R_{\text{lo}})(b-1)/N + \log_{10}(R_{\text{lo}}) \tag{4}$$

where R_{hi} is 300 nWcm^{-2} sr^{-1}, R_{lo} is 5 nWcm^{-2} sr^{-1}, N is the number of bins (*20*), and b is the bin number (from 1 to 20). The range of 5 to 300 nWcm^{-2} sr^{-1} was chosen on the basis of previous experience examining the night light composites. The 5 nWcm^{-2} sr^{-1} cut is far above the instrument sensitivity limit and noise level but still low enough to include the lights from many faintly lit communities. In the October 2012 composite, not a single pixel of Paris was brighter than 300 nWcm^{-2} sr^{-1} (the brightest was 230 nWcm^{-2} sr^{-1} at Charles De Gaulle Airport), and both Los Angeles, California and London, UK had only a single pixel brighter than 300 nWcm^{-2} sr^{-1}. The rare exceptions of brighter urban areas (for example, the Las Vegas strip) are better studied individually than as part of a global analysis.

The radiance bins for each pixel were stored in a Python array of equivalent size to the DNB data (from 60°S to 60°N). To reject wildfires and other temporary lights from the stable light radiance change analysis, we also checked the radiance of each pixel in the October composites for 2013–2015. Pixels were flagged to be removed from the analysis if their radiance was outside the range of 1.67 to 900 nWcm^{-2} sr^{-1} in any of these years. In practice, this was accomplished by setting the bin number of these pixels to 0 in the Python array. At this stage, a set of binary (lit/unlit) maps was also produced for each year from 2012 to 2016 by testing whether each pixel was above the 5 nWcm^{-2} sr^{-1} cut (Fig. 6). The area above the threshold was summed on both the global and national scales.

The radiance ratio R_{2016}/R_{2012} was then calculated for each of the individual pixels with bin numbers in the range of 1 to 20. Pixels that changed by greater than a factor of 4 were removed from the analysis. The value of 4 was chosen as large enough to accommodate most changes in rapidly brightening countries while still rejecting extreme changes to prevent them from skewing the mean (Fig. 7). The area-corrected mean radiance difference D_b for each bin b was then

$$D_b = \frac{\sum wR_{2016}}{\sum wR_{2012}} \tag{5}$$

with a pixel area correction $w = A/\bar{A}_b$, where A is the area of each pixel and $\bar{A}_b$ is the area of the average pixel in each bin. Only pixels that passed all cuts were included in the sums.

The analysis was repeated for each country by recalculating $\bar{A}_b$ and D_b for only the pixels within the given country's area. Country extents were converted from the shapefiles of Esri Data & Maps 2003 to a raster format, with a few corrections to reflect new boundaries (for example, South Sudan). Overseas territories were included as part of the larger associated country (for example, Christmas Island was included as part of Australia). Some coastal pixels are misidentified as oceans because of the limited precision of the shapefile and, therefore, do not contribute to country totals. For countries with lit areas below several square kilometers, caution should be taken when interpreting the change in radiance in figs. S4 to S27 because these changes are driven by a small number of pixels.

Changes in national sum of lights for areas included in the total radiance change analysis were compared to GDP and population data from the World Bank (*44*). GDP is reported in "constant 2010 US$." A total of 134 countries had complete GDP and population data, as well as at least 100 km^2 lit above the 5 nWcm^{-2} sr^{-1} threshold in both 2012 and 2016. Countries were divided in roughly equal groups based on per capita GDP in 2016 for display (Fig. 4A). The per capita GDPs of the groups are <$2000 ($n$ = 36, red triangles), from $2000 to $6000 ($n$ = 35, green squares), from $6000 to $17,000 ($n$ = 30, blue stars), and >$17,000 ($n$ = 33, black circles). Spearman's rank-order correlation coefficients between sets of parameters were calculated in Python using "scipy.stats.spearmanr."

The 5 nWcm^{-2} sr^{-1} threshold means that not all artificially produced light was included in these analyses. Away from cities, natural light sources, such as airglow and reflected moonlight outshine artificial light, and systematic errors on the DNB zero point could generate large errors in the national sum of lights for countries with large unlit areas. Further work would therefore be needed to estimate the total global change in artificial radiance (including areas lit below the current analysis threshold).

One of the consequences of the global transition to LED street lighting is a shift in the spectra of artificial night lights (*22*, *45*). So-called "white" LEDs emit a portion of their light at wavelengths below 500 nm (blue), where the DNB is effectively blind (*23*). This means that a street light transition from (orange) high-pressure sodium lamps to (white) LEDs in which surface luminance is held constant results in a decrease in the radiance observed by DNB (Fig. 5C). The measurements of change in lighting reported here are therefore actually lower bounds on the increase of lighting in the human visual range [see the study of Sánchez de Miguel *et al.* (*45*) for a more detailed discussion].

For this reason, decreases in radiance of ~30% could be due to a complete lighting transition from high-pressure sodium to LED lamps rather than a true decrease in visible light. The relationship between the emission spectra of different lighting technologies (even among classes such as "warm white LEDs" or "high-pressure sodium") and the detection efficiencies of broadband sensors (for example, human vision and VIIRS DNB) is complex and will be addressed in detail in a forthcoming paper. From a remote sensing perspective, the situation could be greatly improved if nighttime satellites had color sensitivity (*46*). Nevertheless, the increased luminous efficacy of LEDs means that decreases in city lighting likely indicate decreases in energy consumption. On the other hand, despite the fact that nearly all new outdoor lighting installations make use of LEDs (*47*), new lighting necessarily implies new energy consumption. For this reason, increases in observed radiance are nearly certain to be due to increases in installed visible light and, therefore, raised energy consumption.

SUPPLEMENTARY MATERIALS

Supplementary material for this article is available at http://advances.sciencemag.org/cgi/content/full/3/11/e1701528/DC1

fig. S1. Normalized cumulative radiance distribution for Afghanistan through Ghana.
fig. S2. Normalized cumulative radiance distribution for Greece through Paraguay.
fig. S3. Normalized cumulative radiance distribution for Peru through Zimbabwe.
fig. S4. Lit area (2014) and radiance change (2012–2016) in Afghanistan, Albania, Algeria, Andorra, Antigua and Barbuda, Argentina, and Armenia.
fig. S5. Lit area (2014) and radiance change (2012–2016) in Australia, Austria, Azerbaijan, Bahrain, Bangladesh, Barbados, Belarus, and Belgium.
fig. S6. Lit area (2014) and radiance change (2012–2016) in Belize, Benin, Bhutan, Bolivia, Bosnia and Herzegovina, Botswana, Brazil, and Brunei.
fig. S7. Lit area (2014) and radiance change (2012–2016) in Bulgaria, Burkina Faso, Burundi, Cambodia, Cameroon, Canada, Cape Verde, and Chad.
fig. S8. Lit area (2014) and radiance change (2012–2016) in Chile, China, Colombia, Comoros, Republic of the Congo, Democratic Republic of the Congo, Costa Rica, and Cote d'Ivoire.
fig. S9. Lit area (2014) and radiance change (2012–2016) in Croatia, Cuba, Cyprus, Czech Republic, Denmark, Djibouti, Dominica, and Dominican Republic.
fig. S10. Lit area (2014) and radiance change (2012–2016) in East Timor, Ecuador, Egypt, El Salvador, Equatorial Guinea, Eritrea, Estonia, and Ethiopia.
fig. S11. Lit area (2014) and radiance change (2012–2016) in Fiji, Finland, France, Gabon, Gaza Strip, Georgia, Germany, and Ghana.
fig. S12. Lit area (2014) and radiance change (2012–2016) in Greece, Grenada, Guatemala, Guinea, Guinea-Bissau, Guyana, Haiti, and Honduras.
fig. S13. Lit area (2014) and radiance change (2012–2016) in Hungary, India, Indonesia, Iran, Iraq, Ireland, Israel, and Italy.
fig. S14. Lit area (2014) and radiance change (2012–2016) in Jamaica, Japan, Jordan, Kazakhstan, Kenya, Kosovo, Kuwait, and Kyrgyzstan.
fig. S15. Lit area (2014) and radiance change (2012–2016) in Laos, Latvia, Lebanon, Lesotho, Liberia, Libya, Liechtenstein, and Lithuania.
fig. S16. Lit area (2014) and radiance change (2012–2016) in Luxembourg, Macedonia, Madagascar, Malawi, Malaysia, Maldives, Mali, and Malta.
fig. S17. Lit area (2014) and radiance change (2012–2016) in Marshall Islands, Mauritania, Mauritius, Mexico, Moldova, Monaco, Mongolia, and Montenegro.
fig. S18. Lit area (2014) and radiance change (2012–2016) in Morocco, Mozambique, Myanmar, Namibia, Nauru, Nepal, Netherlands, and New Zealand.
fig. S19. Lit area (2014) and radiance change (2012–2016) in Nicaragua, Niger, Nigeria, North Korea, Norway, Oman, Pakistan, and Panama.
fig. S20. Lit area (2014) and radiance change (2012–2016) in Papua New Guinea, Paraguay, Peru, Philippines, Poland, Portugal, Qatar, and Romania.
fig. S21. Lit area (2014) and radiance change (2012–2016) in Russia, Rwanda, Samoa, San Marino, Sao Tome and Principe, Saudi Arabia, Senegal, and Serbia and Montenegro.
fig. S22. Lit area (2014) and radiance change (2012–2016) in Seychelles, Sierra Leone, Singapore, Slovakia, Slovenia, Solomon Islands, Somalia, and South Africa.
fig. S23. Lit area (2014) and radiance change (2012–2016) in South Korea, South Sudan, Spain, Sri Lanka, St. Kitts and Nevis, St. Lucia, St. Vincent and the Grenadines, and Sudan.
fig. S24. Lit area (2014) and radiance change (2012–2016) in Suriname, Swaziland, Sweden, Switzerland, Syria, Taiwan, Tajikistan, and Tanzania.
fig. S25. Lit area (2014) and radiance change (2012–2016) in Thailand, The Bahamas, The Gambia, Togo, Trinidad and Tobago, Tunisia, Turkey, and Turkmenistan.
fig. S26. Lit area (2014) and radiance change (2012–2016) in Uganda, Ukraine, United Arab Emirates, UK, the United States, Uruguay, Uzbekistan, and Vanuatu.
fig. S27. Lit area (2014) and radiance change (2012–2016) in Vatican City, Venezuela, Vietnam, West Bank, Western Sahara, Yemen, Zambia, and Zimbabwe.
fig. S28. Annual changes in lit area and total radiance.

REFERENCES AND NOTES

1. R. Fouquet, P. J. Pearson, Seven centuries of energy services: The price and use of light in the United Kingdom (1300–2000). *Energy J.* **27**, 139–177 (2006).
2. J. Y. Tsao, P. Waide, The world's appetite for light: Empirical data and trends spanning three centuries and six continents (2008). *Leukos* **6**, 259–281 (2010).
3. J. Y. Tsao, H. D. Saunders, J. R. Creighton, M. E. Coltrin, J. A. Simmons, Solid-state lighting: An energy-economics perspective. *J. Phys. D Appl. Phys.* **43**, 354001 (2010).
4. F. Hölker, T. Moss, B. Griefahn, W. Kloas, C. C. Voigt, D. Henckel, A. Hänel, P. Kappeler, S. Völker, A. Schwope, S. Franke, D. Uhrlandt, R. Klenke, J. Fischer, C. Wolter, K. Tockner, The dark side of light: A transdisciplinary research agenda for light pollution policy. *Ecol. Soc.* **15**, 13 (2010).
5. F. Falchi, P. Cinzano, D. Duriscoe, C. C. M. Kyba, C. D. Elvidge, K. Baugh, B. A. Portnov, N. A. Rybnikova, R. Furgoni, The new world atlas of artificial night sky brightness. *Sci. Adv.* **2**, e1600377 (2016).
6. K. J. Gaston, M. E. Visser, F. Hölker, The biological impacts of artificial light at night: The research challenge. *Philos. Trans. R. Soc. B* **370**, 20140133 (2015).
7. K. W. Riegel, Light pollution. *Science* **179**, 1285–1291 (1973).
8. American Medical Association, AMA adopts guidance to reduce harm from high intensity street lights (2016); www.ama-assn.org/ama-adopts-guidance-reduce-harm-high-intensity-street-lights [accessed 27 January 2017].
9. A. K. Jägerbrand, New framework of sustainable indicators for outdoor LED (light emitting diodes) lighting and SSL (solid state lighting). *Sustainability* **7**, 1028–1063 (2015).
10. R. Steinbach, C. Perkins, L. Tompson, S. Johnson, B. Armstrong, J. Green, C. Grundy, P. Wilkinson, P. Edwards, The effect of reduced street lighting on road casualties and crime in England and Wales: Controlled interrupted time series analysis. *J. Epidemiol. Community Health* **69**, 1118–1124 (2015).
11. M. Aubé, J. Roby, Sky brightness levels before and after the creation of the first International Dark Sky Reserve, Mont-Mégantic Observatory, Québec, Canada. *J. Quant. Spectrosc. Radiat. Transf.* **139**, 52–63 (2014).
12. P. Pust, P. J. Schmidt, W. Schnick, A revolution in lighting. *Nat. Mater.* **14**, 454–458 (2015).
13. C. Elvidge, M. Imhoff, K. Baugh, V. Hobson, I. Nelson, J. Safran, J. Dietz, B. Tuttle, Night-time lights of the world: 1994–1995. *ISPRS J. Photogramm. Remote Sens.* **56**, 81–99 (2001).
14. C. D. Elvidge, D. Ziskin, K. E. Baugh, B. T. Tuttle, T. Ghosh, D. W. Pack, E. H. Erwin, M. Zhizhin, A fifteen year record of global natural gas flaring derived from satellite data. *Energies* **2**, 595–622 (2009).
15. S. D. Miller, W. Straka, S. P. Mills, C. D. Elvidge, T. F. Lee, J. Solbrig, A. Walther, A. K. Heidinger, S. C. Weiss, Illuminating the capabilities of the Suomi National Polar-Orbiting Partnership (NPP) Visible Infrared Imaging Radiometer Suite (VIIRS) day/night band. *Remote Sens.* **5**, 6717–6766 (2013).
16. J. Proville, D. Zavala-Araiza, G. Wagner, Night-time lights: A global, long term look at links to socio-economic trends. *PLOS ONE* **12**, e0174610 (2017).
17. Q. Huang, X. Yang, B. Gao, Y. Yang, Y. Zhao, Application of DMSP/OLS nighttime light images: A meta-analysis and a systematic literature review. *Remote Sens.* **6**, 6844–6866 (2014).
18. A. Sánchez de Miguel, J. Zamorano, J. G. Castaño, S. Pascual, Evolution of the energy consumed by street lighting in Spain estimated with DMSP-OLS data. *J. Quant. Spectrosc. Radiat. Transf.* **139**, 109–117 (2014).
19. J. Bennie, T. W. Davies, J. P. Duffy, R. Inger, K. J. Gaston, Contrasting trends in light pollution across Europe based on satellite observed night time lights. *Sci. Rep.* **4**, 3789 (2014).
20. F.-C. Hsu, K. E. Baugh, T. Ghosh, M. Zhizhin, C. D. Elvidge, DMSP-OLS radiance calibrated nighttime lights time series with intercalibration. *Remote Sens.* **7**, 1855–1876 (2015).
21. X. Li, Y. Zhou, A stepwise calibration of global DMSP/OLS stable nighttime light data (1992–2013). *Remote Sens.* **9**, 637 (2017).

22. F. Falchi, P. Cinzano, C. D. Elvidge, D. M. Keith, A. Haim, Limiting the impact of light pollution on human health, environment and stellar visibility. *J. Environ. Manag.* **92**, 2714–2722 (2011).
23. C. C. M. Kyba, S. Garz, H. Kuechly, A. Sánchez de Miguel, J. Zamorano, J. Fischer, F. Hölker, High-resolution imagery of Earth at night: New sources, opportunities and challenges. *Remote Sens.* **7**, 1–23 (2015).
24. W. Jiang, G. He, T. Long, H. Liu, Ongoing conflict makes Yemen dark: From the perspective of nighttime light. *Remote Sens.* **9**, 798 (2017).
25. C. Small, C. D. Elvidge, D. Balk, M. Montgomery, Spatial scaling of stable night lights. *Remote Sens. Environ.* **115**, 269–280 (2011).
26. C. Small, C. D. Elvidge, Night on Earth: Mapping decadal changes of anthropogenic night light in Asia. *Int. J. Appl. Earth Obs. Geoinf.* **22**, 40–52 (2013).
27. H. U. Kuechly, C. C. M. Kyba, T. Ruhtz, C. Lindemann, C. Wolter, J. Fischer, F. Hölker, Aerial survey of light pollution in Berlin, Germany, and spatial analysis of sources. *Remote Sens. Environ.* **126**, 39–50 (2012).
28. C. N. H. Doll, J.-P. Muller, C. D. Elvidge, Night-time imagery as a tool for global mapping of socioeconomic parameters and greenhouse gas emissions. *AMBIO* **29**, 157–162 (2000).
29. W. Nordhaus, X. Chen, A sharper image? Estimates of the precision of nighttime lights as a proxy for economic statistics. *J. Econ. Geogr.* **15**, 217–246 (2014).
30. M. Aubé, Physical behaviour of anthropogenic light propagation into the nocturnal environment. *Philos. Trans. Roy. Soc. B Biol. Sci.* **370**, 20140117 (2015).
31. Z. Kolláth, A. Dömény, K. Kolláth, B. Nagy, Qualifying lighting remodelling in a Hungarian city based on light pollution effects. *J. Quant. Spectrosc. Radiat. Transf.* **181**, 46–51 (2016).
32. B. Kinzey, T. E. Perrin, N. J. Miller, M. Kocifaj, M. Aubé, H. S. Lamphar, "An investigation of LED street lighting's impact on sky glow" (Technical Report PNNL-26411, U.S. Department of Energy, 2017).
33. C. C. M. Kyba, A. Hänel, F. Hölker, Redefining efficiency for outdoor lighting. *Energ. Environ. Sci.* **7**, 1806–1809 (2014).
34. N. Narendran, J. P. Freyssinier, Y. Zhu, Energy and user acceptability benefits of improved illuminance uniformity in parking lot illumination. *Light. Res. Technol.* **48**, 789–809 (2016).
35. F. Hölker, C. Wolter, E. K. Perkin, K. Tockner, Light pollution as a biodiversity threat. *Trends Ecol. Evol.* **25**, 681–682 (2010).
36. F. Hölker, C. Wurzbacher, C. Weißenborn, M. T. Monaghan, S. I. J. Holzhauer, K. Premke, Microbial diversity and community respiration in freshwater sediments influenced by artificial light at night. *Philos. Trans. Roy. Soc. B Biol. Sci.* **370**, 20140130 (2015).
37. R. H. ffrench-Constant, R. Somers-Yeates, J. Bennie, T. Economou, D. Hodgson, A. Spalding, P. K. McGregor, Light pollution is associated with earlier tree budburst across the United Kingdom. *Proc. R. Soc. B* **283**, 20160813 (2016).
38. A. Keshet-Sitton, K. Or-Chen, E. Huber, A. Haim, Illuminating a risk for breast cancer: A preliminary ecological study on the association between streetlight and breast cancer. *Integr. Cancer Ther.* 1534735416678983 (2016).
39. C. D. Elvidge, K. Baugh, M. Zhizhin, F. C. Hsu, T. Ghosh, VIIRS night-time lights. *Int. J. Remote Sens.* **38**, 5860–5879 (2017).
40. J. Nelson, Lights on & lights out; https://adventuresinmapping.com/2017/04/18/lights-on-lights-out/ [accessed 25 June 2017].
41. National Centers for Environmental Information, National Oceanic and Atmospheric Administration, Version 1 VIIRS Day/Night Band Nighttime Lights; www.ngdc.noaa.gov/eog/viirs/download_dnb_composites.html [accessed 17 April 2017].
42. N. Levin, Q. Zhang, A global analysis of factors controlling VIIRS nighttime light levels from densely populated areas. *Remote Sens. Environ.* **190**, 366–382 (2017).
43. Z. Wang, X. Xiong, J. Fulbright, N. Lei, VIIRS day/night band radiometric calibration stability monitoring using the Moon. *J. Geophys. Res. Atmos.* **122**, 5616–5624 (2017).
44. World Bank, World Development Indicators May 2017 Edition; http://data.worldbank.org [accessed 21 September 2017].
45. A. Sánchez de Miguel, M. Aubé, J. Zamorano, M. Kocifaj, J. Roby, C. Tapia, Sky quality meter measurements in a colour-changing world. *Mon. Not. R. Astron. Soc.* **467**, 2966–2979 (2017).
46. C. D. Elvidge, P. Cinzano, D. R. Pettit, J. Arvesen, P. Sutton, C. Small, R. Nemani, T. Longcore, C. Rich, J. Safran, J. Weeks, S. Ebener, The Nightsat mission concept. *Int. J. Remote Sens.* **28**, 2645–2670 (2007).
47. Northeast Group LLC, "Global LED and smart street lighting: Market forecast (2016–2026)" (Technical Report 4033593, 2016).
48. A. Sánchez de Miguel, J. G. Castaño, J. Zamorano, C. C. M. Kyba, S. Pascual, M. Ángeles, L. Cayuela, G. Martín Martinez, P. Challupner, Atlas of astronaut photos of Earth at night. *Astron. Geophys.* **55**, 4.36 (2014).

Acknowledgments: We thank the anonymous reviewers for a number of helpful suggestions. This article is based on work from COST (European Cooperation in Science and Technology) Action ES1204 LoNNe (Loss of the Night Network), supported by COST. **Funding:** The authors acknowledge the funding received by ERA-PLANET (www.era-planet.eu) funded by the European Commission as part of H2020 (Horizon 2020) (H2020) (contract no. 689443). NOAA's participation was funded by NASA's VIIRS science program (contract number NNH15AZ01I). A.S.d.M.'s contribution was funded by ORISON project (H2020-INFRASUPP-2015-2) Cities at Night. Image and data processing was performed by NOAA's National Geophysical Data Center. Figs. 1, 2, and 5 were created using ArcGIS software by Esri. **Author contributions:** C.C.M.K., T.K., A.S.d.M., A.J., F.H., J.B., K.J.G., and L.G. conceived the study; A.S.d.M. independently verified some results; C.C.M.K., T.K., and C.D.E. provided the figures; A.J. prepared the Supplementary Materials; K.B. and C.D.E. created the monthly DNB composites and provided assistance in interpreting them; C.C.M.K. wrote the first draft; and all authors edited and approved the draft manuscripts. **Competing interests:** All authors declare that they have no competing interests; however, in the interest of full disclosure, C.C.M.K. (2012–2015) and A.S.d.M. (2016 to present) note that they have served as uncompensated members of the board of directors of the International Dark-Sky Association. **Data and materials availability:** All data needed to evaluate the conclusions in the paper are present in the paper and/or the Supplementary Materials. Additional data related to this paper may be requested from the authors.

Submitted 9 May 2017
Accepted 24 October 2017
Published 22 November 2017
10.1126/sciadv.1701528

Citation: C. C. M. Kyba, T. Kuester, A. Sánchez de Miguel, K. Baugh, A. Jechow, F. Hölker, J. Bennie, C. D. Elvidge, K. J. Gaston, L. Guanter, Artificially lit surface of Earth at night increasing in radiance and extent. *Sci. Adv.* **3**, e1701528 (2017).

ScienceAdvances

Artificially lit surface of Earth at night increasing in radiance and extent

Christopher C. M. Kyba, Theres Kuester, Alejandro Sánchez de Miguel, Kimberly Baugh, Andreas Jechow, Franz Hölker, Jonathan Bennie, Christopher D. Elvidge, Kevin J. Gaston and Luis Guanter

Sci Adv **3** (11), e1701528.
DOI: 10.1126/sciadv.1701528